



# Effect of chemical, mineralogical, and petrographic properties on the grindability of a South African Highveld coal

R. Matjie<sup>1</sup>, J. Bunt<sup>1</sup>, A. Goosen<sup>1</sup>, K. Mphahlele<sup>1</sup>, and R. Uwaoma<sup>2</sup>

## Affiliation:

<sup>1</sup>Centre of Excellence in Carbon-Based Fuels, School of Chemical and Minerals Engineering, North-West University, Potchefstroom, South Africa.

<sup>2</sup>School of Physical and Chemical Sciences, North-West University, Potchefstroom, South Africa.

Correspondence to:  
R. Matjie

Email:  
matjie4@gmail.com

## Dates:

Received: 25 Oct. 2021

Revised: 17 Oct. 2022

Accepted: 17 Oct. 2022

Published: July 2023

## How to cite:

Matjie, R., Bunt, J., Goosen, A., Mphahlele, K., and Uwaoma, R. 2023

Effect of chemical, mineralogical, and petrographic properties on the grindability of a South African Highveld coal.

Journal of the Southern African Institute of Mining and Metallurgy, vol. 123, no. 7, pp. 381-390

## DOI ID:

<http://dx.doi.org/10.17159/2411-9717/2423/2023>

## ORCID:

R. Matjie

<http://orcid.org/0000-0002-2839-3729>

J. Bunt

<http://orcid.org/0000-0003-3051-2528>

A. Goosen

<http://orcid.org/0009-0005-2731-0986>

R. Uwaoma

<http://orcid.org/0000-0002-3306-9878>

## Synopsis

Coal properties that are associated with wear and damage of grinding equipment during pulverization prior to combustion were investigated. A South African Highveld feed coal and its beneficiated fractions were crushed to <1 >0.25 mm particles for the grindability tests. These particles were milled and screened into <75  $\mu\text{m}$  and >75  $\mu\text{m}$  fractions, which were analysed by different techniques to establish a correlation with the conventional Hardgrove Grindability Index (HGI). The <1.5 g.cm<sup>-3</sup> float fraction, which contained 93 vol.% (mineral matter free) total-macerals, 9% kaolinite, and had the lowest HGI (57) (hardest to grind) was pulverized for 15, 30, 60, and 120 minutes for particle size distribution analysis. This analysis indicated that the content of <75  $\mu\text{m}$  particles increases with increased grinding time. The >1.9 g.cm<sup>-3</sup> sink fraction, with the highest HGI (76), 44% kaolinite, and 20 vol.% total macerals, was ground easily to generate the highest proportion of <75  $\mu\text{m}$  particles. Based on higher correlation coefficients ( $R^2 = 0.77-0.91$ ), the ash yield, mineral matter, petrographic composition, and fixed-carbon have significant effects on the HGI. Conversely, the inherent moisture and total sulphur ( $R^2 = 0.48-0.62$ ) have only minor effects on the HGI. Results from this investigation could be implemented in the preparation of a suitable pulverized fuel with little equipment wear, as well as utilizing mineralogical and petrographic compositions. Finally, the effect of microlithotypes and maceral types in South African feed coals on the HGI should be investigated in further pulverization and grindability studies.

## Keywords

coal, mineralogy, petrography, grindability, Hardgrove Index.

## Introduction

South African power stations utilize low-rank C bituminous coal for electricity and steam production (Falcon and Falcon, 1987; Falcon and Ham, 1988; Borrego, Alvarez, and Menéndez, 1997). These coarse run-of-mine (ROM) coals (<120 to >6.7 mm particle size) are ground to produce pulverized fuel (PF) (<75  $\mu\text{m}$  particles) for combustion (Falcon and Falcon, 1987). The Grootegeluk opencast coal mine owned by Kumba Resources (Pty) Ltd, situated west of Lephalale in Limpopo Province, produces very coarse ROM coal (1000 mm, 55-60% ash yield) (Jeffrey, 2005). At Grootegeluk, primary crushers are utilized to reduce these large lumps to <150 mm particles without producing excessive fines. This material is then beneficiated to yield various products (semi-soft coking coal, high-ash steam coal (middlings, 35%), Corex coal, medium-phosphorus pulverized coal injection (PCI) coal, and sized steam coal). The bulk of the beneficiated high-ash coal (14.2 Mt/a) is transported by conveyor to Eskom's Matimba and Medupe power stations to produce electricity. If the calorific value (CV) and percentage ash yield do not meet requirements for combustion, this coal is blended with low-ash coking coal (6-15% ash yield) to produce a suitable combustion PF with a  $\leq 35\%$  ash yield (air dry basis (a.d.b)), <0.5-1% total sulphur (a.d.b), 40-55% fixed-carbon (a.d.b), and CV (15-25 MJ/kg)) with low equipment wear propensity.

According to Falcon and Falcon (1987), vitrinite macerals contained in SA low-rank coals impart a Hardgrove Grindability Index (HGI) value of 24 and these coals are very difficult to grind due to their elastic behaviour. While vitrinite macerals present in mid- to high-rank bituminous coals (HGI value of 84) are easiest to grind, grindability decreases again in the anthracite range. The HGI values of inertinite

# Effect of chemical, mineralogical, and petrographic properties

(45–50) vary slightly in low-rank bituminous coals, including South Africa coals, and remain consistent throughout the bituminous and semi-anthracite range (Steyn and Minnitt, 2010, Mangena, 2001, Engelbrecht *et al.*, 2010).

Studies on South African coals have shown that three factors – the inherent moisture content, percentage ash yield, and volatile matter content – greatly influence the HGI (van Vuuren, 1978; Falcon and Falcon, 1987). Coals with lower HGI values have high inherent moisture and volatile matter contents along with low ash yields.

Grinding of coal incurs a significant energy cost (5 to 15 kWh/t– (Sligar 1998; Khoshjavan, Khoshjavan, and Reza, 2013). The presence of mineral matter, including quartz, pyrite, and microcline in the coal particles, which are harder than steel, can contribute significantly to equipment wear during pulverization or milling (Falcon and Falcon, 1987; Tiryaki and Dikmen, 2005; Deniz, 2011). The extraneous or discrete minerals in the coals are those minerals which are not associated with the carbon matrix. These minerals damage equipment, decreasing its operational lifespan and subsequently resulting in power station or boiler shutdowns, and increased costs for repairs or purchasing new equipment.

Furthermore, Honaker, Mohanty, and Crelling (1996) and Vranjes *et al.* (2018) found that vitrinite and liptinite (reactive macerals) and inertinite (inert maceral) behave differently due to their elastic and microhardness properties during grinding and pulverization of Illinois No. 6 seam and Ukrainian coals respectively. Determination of coal maceral microhardness could possibly define the behaviour of Indian coals during grinding/pulverization (Nag *et al.*, 2022).

Trimble and Hower (2003) found that the proportions of liptinite and liptinite-rich microlithotypes in the Eastern Kentucky coals significantly influence the HGI due to their hardness and resistance to grinding. Additionally, the coal rank (0.75–1.00% vitrinite reflectance maximum,  $R_{max}$ ) as well as vitrinite-, liptinite-, and kaolinite-rich mono- and bimaceral monomacrerite affect HGI values. According to Hansen and Hower (2014) and Hower, Graese, and Klapheke (1987), the bimacerite, duroclarite, clarodurite, the bimacerite microlithotype durite, and monomacrerite microlithotype, and liptite in coal negatively contribute to HGI. This implies that coals with these lithotypes require a greater energy input to grind. The monomacrerite microlithotype vitrite and silicates (generally clays) in the coal samples contribute positively to the HGI (higher HGI values, easier to grind).

Idris *et al.* (2022) measured the HGI values of blends of Malaysian low- and high-grade coals by a bomb grindability index. The cross-validated model was developed using a multilinear regression. This model achieved improved HGI predictions for the coal blends, with a coefficient of determination  $R^2 = 0.9416$ . Hower *et al.* (2021) also used HGI as a predictor of the behaviour of Kentucky and non-Kentucky coals during breakage, grinding operations in coal mining, beneficiation, handling, and pulverization.

Numerous research studies of the relationship between mechanical properties, grindability, and cuttability of coal have concluded that these relationships correlate strongly with the HGI (Tiryaki and Dikmen, 2005). Other factors that influence the HGI are coalification (coal rank), volatile matter, fixed-carbon, moisture, total sulphur, carbon, oxygen, nitrogen, and hydrogen (Khoshjavan, Khoshjavan, and Reza, 2013). Taking carbon (C) content as an example, if the C content is higher than 60%, the HGI of the coal increases to the maximum range (30–60) (Falcon and Falcon, 1987;

Hansen, and Hower, 2014; Khoshjavan, Khoshjavan, and Reza, 2013).

Therefore, an improved understanding of the role of these harder minerals, harder macerals, and their composition in South African feed coals during PF comminution for combustion in power stations is needed. The grindability information (optimum grinding time of dry coal particles to produce sized power station feed coal), determined here by assessing density-fractionated samples with different proportions of mineral matter, macerals, chemicals, and microlithotypes, which has not been previously investigated using this novel grindability procedure, may enable operators to better estimate wear rates of susceptible equipment as well as to enhance production efficiencies. The results from this study could also be implemented by research institutions to further investigate the effects of the types of macerals and microlithotypes on the HGI of South African coals from the different coalfields.

In this study, the effects of petrology and mineralogical properties on the grindability and particle size distribution (PSD) of Highveld feed coal and its density-separated fractions were investigated. X-ray diffraction (XRD), X-ray fluorescence (XRF), proximate, petrographic, HGI, and ultimate analyses of the feed coal and its density-separated fractions were undertaken. Furthermore, mineralogical and Malvern Mastersizer analyses of the samples were used to correlate coal properties with the grindability (HGI values) of the coals.

## Materials and methods

### Coal sampling, preparation, density separation and methods

The Highveld Coalfield is situated in South Africa's Mpumalanga Province, where low-medium rank C bituminous coal of Permian age is mined from two economic seams (Falcon and Falcon, 1987; Falcon and Ham, 1988). In this study, approximately 600 kg of a representative Highveld feed coal was sampled at an operating colliery following the International Organization for Standardization (ISO) 18283 and ISO 13909-4 procedures.

A density fractionation method using 1.5 g.cm<sup>-3</sup> to 1.9 g.cm<sup>-3</sup> organic dense media (mixtures of tetrabromoethane, perchloroethylene, and benzene) was followed to produce different density-separated fractions from the <120 >6.7 mm feed coal used in this study, as also applied by Rautenbach *et al.* (2019). The density fractionation work was conducted at General Society of Surveillance (SGS) laboratories' according to the SANS/ISO 7936 method.

The cumulative mass percentage curve is presented in Figure 1. It is apparent that the density separation was successful in producing samples for the HGI measurements at SGS laboratories and grindability tests. As expected, the cumulative mass of the density-separated fractions increases with an increase in the density of the organic liquids, and this data was used to determine a blending strategy to produce a suitable combustion PF.

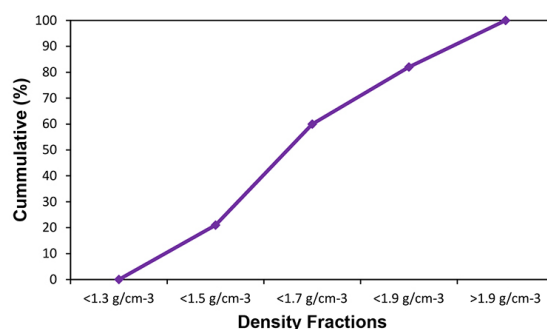


Figure 1—Cumulative mass % of the feed coal's density-separated fractions

# Effect of chemical, mineralogical, and petrographic properties

Prior to pulverization and density separation, representative samples were submitted for HGI analysis at the SGS laboratories in Secunda. The remaining feed coal and density-separated fractions were ground and pulverized to prepare samples (<75, <212, and >250<1000 µm particles) for the selected analyses.

## Coal grindability experimental procedure

A schematic diagram showing the coal sampling, preparation, density separation, grindability experimental procedure and analytical methods for Highveld coal and density-separated fractions is presented in Figure 2.

Each sample (2 kg) of either coarse feed coal or coarse density-separated fraction was hammer milled to produce a size fraction >250<1000 µm for the grindability experiments. The air dried particles (about 100 g) were added into the stainless-steel ball mill and were milled for 60 minutes. Each sample was weighed before and after to ensure that no loss of sample occurred during milling. The grindability test was conducted five times to test the replication of the experimental results. The milled dry sample (about 1 g) was taken for the PSD determination prior to wet screening.

50 g of the milled air dried particles were wet screened using a 75 µm sieve and 2 L water to produce both ground coarser (>75 µm) wet-cake and a finer (<75 µm) coal slurry. The slurry was pressure filtered to separate the wet solids (<75 µm particles). These solids as well as the coarser screened particles (>75 µm) were dried at 60 °C for 4 hours and weighed.

From the wet screening results, it was found that the <1.5 g.cm<sup>-3</sup> float fraction contained the lowest percentage mass of the finer (<75 µm) coal particles due to its high content of vitrinite which is hard to grind (Table V). Also, the lowest HGI value (56.5) was for the <1.5 g.cm<sup>-3</sup> float fraction (Figure 5). Thus, this density fraction was used for the optimization experiments. In each experiment, a 100 g sample of the dry <1.5 g.cm<sup>-3</sup> float fraction was subjected to ball milling for 15, 30, 60, and 120 minutes. The optimization experiment was conducted in duplicate to test the replication of the results. The sample was weighed before and after milling (before wet screening tests) and 1 g of each air dried milled sample was submitted for the PSD analysis using the Malvern mastersizer 3000.

## Proximate analysis and calorific value (CV) measurement

Standard procedures were used to determine the percentage ash yield (ISO 1171), inherent moisture (ISO 11722), and volatile matter content (ISO 562 and 1170) of the samples as well as the CV measurement at SGS laboratories. The fixed-carbon content in each sample was calculated by difference (100 minus the sum of percentage ash yield, inherent moisture, and volatile matter contents).

## Ultimate analyses

The ultimate analysis (ISO 12902-CHN instrumental method) was followed to determine the proportions of organic elements (C, H, N) in the feed coal and density-separated fractions at SGS laboratories. In addition, the ASTM D4239 standard method was used to measure the total sulphur content by the A632 sulphur determinator.

## Sulphur speciation and total sulphur analysis

The feed coal and density-separated fractions were submitted to SGS Laboratories in Trichardt for the sulphur analyses. The ISO 157 method, Standard Part 11, 1959, was followed to quantify the different sulphur forms (pyritic, sulphate, and organic) as well as mineral sulphur (the sum of pyritic and sulphatic sulphur).

## XRF analysis

XRF analysis (Norrish and Hutton, 1969; ASTM D4326-13) was followed to determine the proportions of inorganic elements contained in the ashes of the feed coal, the density fractions, and samples produced from the grindability experiments, using a PANalytical Axios MAX XRF instrument at North-West University (NWU) Potchefstroom campus.

## XRD analysis

The pulverized feed coal, density fractions, and coal samples from experiments (<75 µm) were analysed using a PANalytical X'Pert Pro X-ray diffraction (XRD) instrument equipped with a Co X-ray tube and X'Celerator detector, with Rietveld-based X'Pert

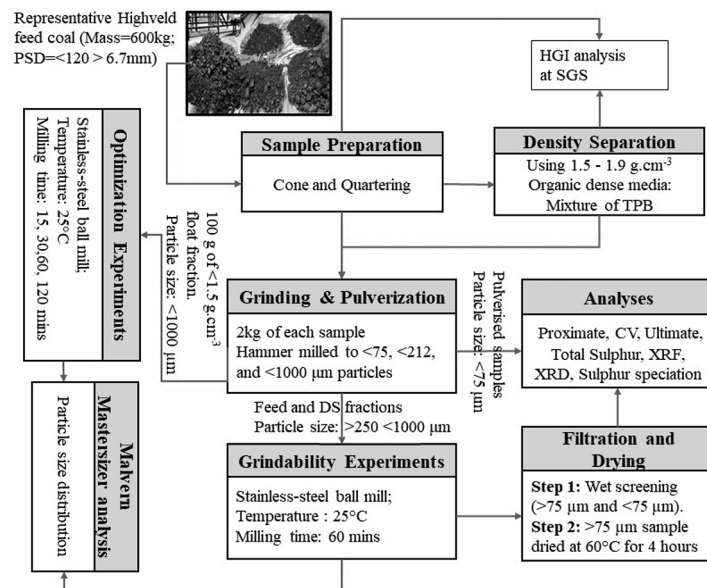


Figure 2 — Schematic diagram of coal sample preparation, density separation, coal grindability experimental procedure and analytical methods. Note: TPB = Mixture of tetrabromoethane, perchloroethylene and benzene, DS fractions = Density-separated fractions

# Effect of chemical, mineralogical, and petrographic properties

HighScore Plus software at NWU Potchefstroom campus (Rietveld, 1969; Speakman, 2012). Each solid sample was spiked with 20% Si (Aldrich, 99.9% purity) and subsequently micronized in a McCrone micronizing mill. Crystalline and amorphous phases were identified and quantified using X'Pert Highscore Plus and an ICDD (International Centre for Diffraction Data) program. Quantification of the phases was based on the Rietveld method.

## HGI analysis

The feed coal and density fractions were submitted to SGS laboratories, Trichardt, for HGI measurement following the ISO 5074:1994 standard method.

## Petrographic analysis

Polished blocks of feed coal and beneficiated fractions were assessed using a Zeiss Axio Imager petrographic microscope fitted with a fossil Hilgers system for vitrinite reflectance determination (based on ISO7404 part 3), housed at the University of Johannesburg. A semi-automated point counting stage for maceral analysis was utilized in accordance with ISO 7404-4 at 500× magnification under oil immersion. The 0.900 YAG calibration standards were used. Maceral results are reported on a volume per cent basis and macerals are included in the count not determined by calculation. The entire surface of each polished block was assessed.

## PSD analysis

The pulverized coal samples were submitted to NWU laboratories in the Potchefstroom campus for the PSD analysis. A Malvern Instrument Mastersizer 3000 (Malvern Instrument, 2015) was used to determine the PSD of the dry samples produced after the milling tests at the different time intervals, before the wet screening tests.

## Results and discussion

### Coal composition

#### Proximate analysis

As expected, the major differences in the proximate analysis results

of the feed coal and density fractions (on an air-dried basis) are the percentage ash yield and fixed-carbon content (Table I). The  $>1.9 \text{ g.cm}^{-3}$  sink fraction has the highest ash yield (74% a.d.b) and the lowest fixed-carbon content (12% a.d.b) of all the samples, including the feed coal. The ash yield increases from the lowest density fraction ( $<1.5 \text{ g.cm}^{-3}$  float fraction) to the highest ( $>1.9 \text{ g.cm}^{-3}$  sink fraction) (Table I). Also, the volatile matter content and the percentage fixed-carbon are higher in the float fractions ( $<1.5 \text{ g.cm}^{-3}$ ,  $<1.7 \text{ g.cm}^{-3}$ , and  $<1.9 \text{ g.cm}^{-3}$  floats) than in the  $>1.9 \text{ g.cm}^{-3}$  sink fraction and feed coal. The  $<1.7 \text{ g.cm}^{-3}$  float sample has a higher ash yield (22% a.d.b) and a lower VM (25% a.d.b), and fixed-carbon content (49% a.d.b) than the  $<1.5 \text{ g.cm}^{-3}$  float sample (used to produce good quality PF). The results from earlier studies indicate that coals with high ash yields and higher moisture content had high HGI values (Shahzad *et al.*, 2014 (a); Shahzad *et al.*, 2014 (b); Babu, Lawrence, and Sivashanmugam, 2017). This implies that the coals used in these earlier grindability studies are soft and easy to grind.

Furthermore the  $>1.9 \text{ g.cm}^{-3}$  sink fraction sample (used to produce poor quality PF), with a higher ash yield and lower content of fixed-carbon, could possibly be ground with ease.

The highest volatile matter and fixed-carbon contents (a.d.b), along with the lowest percentage ash yield, are evident in the  $<1.5 \text{ g.cm}^{-3}$  float fraction, which could be an indicator that this fraction should be the hardest to grind. By inference, the hardness of the  $<1.5 \text{ g.cm}^{-3}$  float fraction may be directly responsible for high equipment wear during the preparation of the fine PF particles for combustion (Tiryaki and Dikmen, 2005).

#### Ultimate analysis

The ultimate analysis results for the feed coal and density fractions are shown in Table I. As expected, lower concentrations of nitrogen and hydrogen along with higher concentrations of carbon were detected in the float samples ( $<1.5 \text{ g.cm}^{-3}$ ,  $<1.7 \text{ g.cm}^{-3}$ ,  $<1.9 \text{ g.cm}^{-3}$ ) and the feed coal sample compared to those of the  $>1.9 \text{ g.cm}^{-3}$  sink fraction. Also, the elemental analysis of the density fractions indicates that the proportions of C, H, and N decrease with increasing particle density. The  $<1.5 \text{ g.cm}^{-3}$  float fraction contains

		Feed coal	$<1.5 \text{ g.cm}^{-3}$ float	$<1.7 \text{ g.cm}^{-3}$ float	$<1.9 \text{ g.cm}^{-3}$ float	$>1.9 \text{ g.cm}^{-3}$ sink
Proximate analysis (% a.d.b) (% a.d.b) (% a.d.b) (% dry, ash-free)	Inherent moisture	3.3	3.8	4.0	2.0	2.1
	Ash	35.9	12.2	22.0	45.9	74.2
	Volatile matter	21.4	27.5	25.1	17.8	11.3
	Fixed-carbon	39.4	56.5	48.9	34.3	12.5
Specific energy (gross, a.d.b)	CV (MJ/kg)	18.7	27.5	24.1	15.4	4.6
Ultimate analysis (% dry, ash-free) (% dry, ash-free) (% dry, ash-free) (% dry, ash-free)	Carbon	47.0	66.8	59.0	40.0	17.8
	Hydrogen	2.8	3.9	3.4	2.3	1.6
	Nitrogen	1.2	1.9	1.5	0.9	0.4
	Oxygen	8.2	11.2	9.9	7.5	2.3
Sulphur (%)	Total sulphur	0.8	0.4	1.1	1.5	1.6
	Sulfate sulphur	0.1	0.0	0.1	0.1	0.0
	Organic sulphur	0.3	0.3	0.3	0.2	0.2
	Pyritic sulphur	0.4	0.1	0.7	1.2	1.4

Note: a.d.b.: air-dried basis

## Effect of chemical, mineralogical, and petrographic properties

the highest volatile matter, which correlates to the contents of carbon, oxygen, nitrogen, and hydrogen. The ultimate results are also comparable with those of the previous studies on Highveld coals (Rautenbach *et al.*, 2019; Matjie *et al.*, 2016).

Khoshjavan, Khoshjavan, and Reza (2013) used an artificial neural network (ANN) method to investigate the effects of other chemical constituents (carbon, nitrogen, oxygen, hydrogen, and total sulphur (organic and pyritic), all on a dry basis) on the HGI of coal. The results for the coals of the same rank from their study show that the carbon, hydrogen, nitrogen, and oxygen contributed significantly to the HGI results. Therefore, the higher proportion of carbon in the  $<1.5 \text{ g.cm}^{-3}$  float fraction could be linked to the microhardness properties of the organic matter during the grindability experiments. This would probably result in wear and damage to plant equipment during the production of PF.

### Total sulphur and sulphur speciation

Total sulphur and sulphur speciation results are presented in Table I. As expected, proportions of pyrite in the density fractions increase with an increase in the density of the organic liquid used for the density separation. This can be attributed to the presence of pyrite that is associated with extraneous rock particles (mudstone, siltstone, and sandstone) in South African feed coals and lithofacies (Faure, Willis, and Dreyer, 1996; Matjie, van Alphen, and Pistorius 2006). The results obtained in this study are also consistent with those from other Highveld coals (Tsemame *et al.*, 2019; Matjie *et al.*, 2018).

The presence of harder minerals such as pyrite can, depending on the particle shape and mode of occurrence in the coal particles, potentially be related to the erosion or wearing of the gasification and combustion process equipment during pulverization (Falcon and Falcon, 1987). In addition, Kogut *et al.* (2021) found that the HGI decreases with an increase in the total sulphur content in Polish coking coals; total sulphur is generally associated with pyrite.

### XRF Analysis

The XRF analysis indicates the inorganic elements present in the ashes of the feed coal and its density fractions (Table II). All inorganic elements are associated with mineral matter (minerals and non-mineral inorganics). Higher proportions of Si and Al are likely associated with kaolinite and microcline in the rock fragments (mudstone, siltstone, and sandstone) identified by the XRD analysis (Tables II and III). Also, a higher proportion of Si is linked to both quartz and clay minerals present in the samples. In previous studies on Highveld coals (Rautenbach *et al.*, 2019), it was observed that there is an increase in Si and Al in the heavier sink fraction. Our XRF results (Table II) are consistent with those results. The ash yield, mineral matter, and inorganic elements contained in the coal samples can affect the grindability (Babu, Lawrence, and Sivashanmugam, 2017).

### XRD Analysis

The XRD analysis of the feed coal and its density-separated fractions indicate that these samples contained significantly high

Table II

Chemical composition of ashes (inorganic elemental oxides) of feed coal and its density-separated fractions (SO<sub>3</sub>- free, wt. %)

Sample	Feed coal	<1.5 g.cm <sup>-3</sup> float	<1.7 g.cm <sup>-3</sup> float	<1.9 g.cm <sup>-3</sup> float	>1.9 g.cm <sup>-3</sup> sink
SiO <sub>2</sub>	55.9	46.0	53.3	61.4	62.7
Al <sub>2</sub> O <sub>3</sub>	25.1	22.8	23.8	24.8	27.0
CaO	8.0	20.0	14.5	5.2	1.6
MgO	2.1	2.8	1.9	1.7	0.8
Fe <sub>2</sub> O <sub>3</sub>	3.9	2.6	2.8	3.4	4.1
P <sub>2</sub> O <sub>5</sub>	1.4	2.0	1.1	0.5	0.3
TiO <sub>2</sub>	1.4	1.7	1.3	2.0	1.5
K <sub>2</sub> O	1.3	1.0	0.8	0.6	1.6
Na <sub>2</sub> O	0.6	0.9	0.3	0.2	0.3
V <sub>2</sub> O <sub>5</sub>	0.1	0.0	0.1	0.1	0.1
MnO	0.1	0.1	0.1	0.1	0.1
Total	100	100.1	100.0	100.1	100.0

Table III

Mineralogical composition of feed coal and density-separated fractions (wt. %)

Sample	Feed coal	<1.5 g.cm <sup>-3</sup> float	<1.7 g.cm <sup>-3</sup> float	<1.9 g.cm <sup>-3</sup> float	>1.9 g.cm <sup>-3</sup> sink
Quartz	9.2	2.5	4.8	21.4	19.7
Kaolinite	19.1	8.6	11.6	25.5	43.6
Pyrite	0.5	0.2	1.8	0.8	1.3
Dolomite	2.7	1.3	6.7	3.4	0.8
Calcite	0.4	0.4	3.5	0.5	0.0
Microcline	0.3	0.3	1.0	0.1	0.6
Illite	0.5	0.1	0.1	0.8	2.6
Rutile	0.2	0.1	0.0	0.1	0.3
Anatase	0.1	0.1	0.0	0.3	0.2
Goyazite	0	0.0	0.0	0.1	0.0
Mineral matter	33	13.6	29.5	53.0	69.1
Amorphous (organic C)	67	86.5	70.5	47.1	30.9
Total	100	100.1	100.0	100.1	100.0

## Effect of chemical, mineralogical, and petrographic properties

proportions of kaolinite, mineral matter and quartz with lesser proportions of dolomite, pyrite, and calcite, and a minor proportion of microcline and traces of illite and anatase (Table III). As the density of the organic liquid decreased, the proportions of quartz and kaolinite significantly decreased in the density-separated fractions (Table III). A higher concentration of amorphous organic carbon significantly decreased in the density-separated fractions as the density of the organic liquid increased. The proportion of mineral matter increased in the density-separated fractions with an increase in the density of the organic liquid. The  $<1.7 \text{ g.cm}^{-3}$  float fraction has the highest proportions of dolomite and calcite compared to density fractions. This implies that the pyrite, quartz, and kaolinite which are associated with the extraneous rock fragments (mudstone, siltstone, and sandstone) are mostly concentrated in the  $>1.9 \text{ g.cm}^{-3}$  sink fraction samples, and inherent pyrite, quartz and kaolinite associated with a small proportion of carbon containing particles. These XRD results are consistent with the XRD data obtained from the previous mineralogical studies on Highveld coal samples (Matjie *et al.*, 2016; Rautenbach *et al.*, 2019).

### Petrographic analysis

The random vitrinite reflectance values ( $R_{oV}\%$ ) of the feed coal and density fractions are presented in Table IV. The vitrinite reflectance analysis indicates that the samples represent medium rank C bituminous coal as per the ECE-UN 1988 in-seam classification scheme. The standard deviation is low. The  $<1.9 \text{ g.cm}^{-3}$  float sample and  $>1.9 \text{ g.cm}^{-3}$  sink sample with high ash yield contained very few collotelinite (vitrinite) particles and hence the samples were not suitable for reflectance analysis. The reflectance results from the other samples ( $<1.5 \text{ g/cm}^{-3}$ ,  $<1.7 \text{ g.cm}^{-3}$ , and feed coal) indicate uniform results for South African coals (Falcon and Falcon, 1987; Borrego, Alvarez, and Menéndez, 1997).

The maceral compositions (reported as percentage by volume) of the feed coal and beneficiated fractions are shown in Table V. Micrographs of the  $<1.5 \text{ g.cm}^{-3}$  float fraction and the  $>1.9 \text{ g.cm}^{-3}$  sink fraction are presented in Figures 3 and 4 respectively. The vitrinite content increased from 15.3 vol.% in the feed coal to 33.3

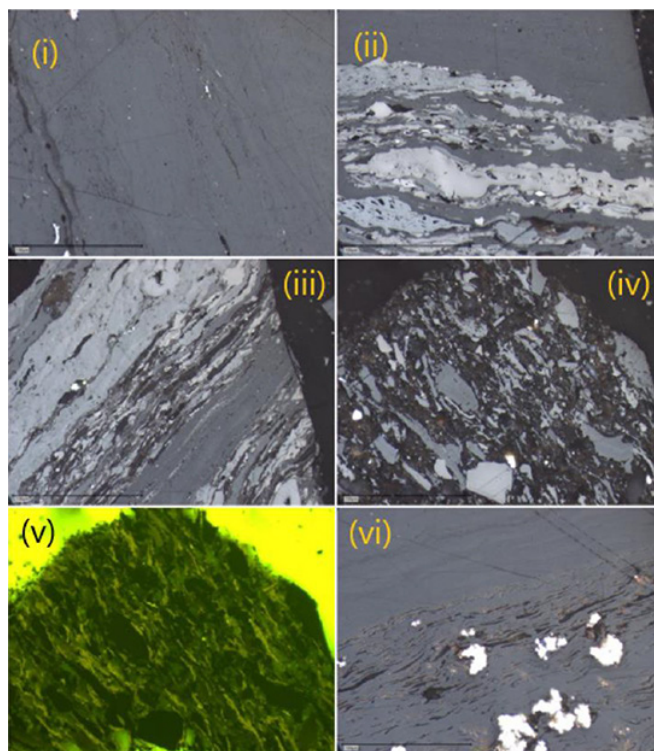


Figure 3—Micrographs of the  $<1.5 \text{ g.cm}^{-3}$  float fraction: (i) vitrinite; (ii) Banded vitrinite and (lighter shade) inertinite, with very small, included quartz minerals; (iii) Banded coal with (dark) liptinite, (medium grey) vitrinite, and (light) inertinite. The image is dominated by inertinite; (iv) Particle enriched in liptinite; (v) Fluorescent image of (iv); (vi) Banded vitrinite with a clean vitrinite band on top and a band of vitrinite with included clays and pyrite (reflected light, oil immersion, x500, scale included 100 microns)

vol.% in the  $<1.5 \text{ g.cm}^{-3}$  float fraction and decreased to 14.2 vol.%, 3.9 vol.%, and 4.5 vol.% in the  $<1.7 \text{ g.cm}^{-3}$  float fraction,  $<1.9 \text{ g.cm}^{-3}$  float fraction, and  $>1.9 \text{ g.cm}^{-3}$  sink fraction respectively as the density of the organic liquid increased. The inertinite content

Table IV

#### Vitrinite reflectance analysis ( $R_{oV}\%$ )

Sample	$<1.5 \text{ g.cm}^{-3}$ float	$<1.7 \text{ g.cm}^{-3}$ float	Feed coal	$<1.9 \text{ g.cm}^{-3}$ float	$>1.9 \text{ g.cm}^{-3}$ sink
Maceral group (mineral matter included)					
Vitrinite reflectance ( $R_{oV}\%$ )	0.6	0.6	0.6	* C too low	*C too low
Standard deviation	0.1	0.1	0.1		
Maximum	0.8	0.8	0.8		
Minimum	0.5	0.5	0.5		
No. of points	108.0	98.0	95.0		
Rank category	M	M	M		

M: Medium rank C; \* C too low: collotelinite too low

Table V

#### Maceral group composition and total minerals of the feed coal and its density-separated fractions (vol. %)

	Feed coal	$<1.5 \text{ g.cm}^{-3}$ float	$<1.7 \text{ g.cm}^{-3}$ float	$<1.9 \text{ g.cm}^{-3}$ float	$>1.9 \text{ g.cm}^{-3}$ sink
Vitrinite	15.3	33.3	14.2	3.9	4.5
Inertinite	53.6	53.6	62.3	56.2	14.1
Liptinite	4	5.9	3.7	1.7	1.2
Mineral matter	27.1	7.2	19.8	38.2	80.2

# Effect of chemical, mineralogical, and petrographic properties

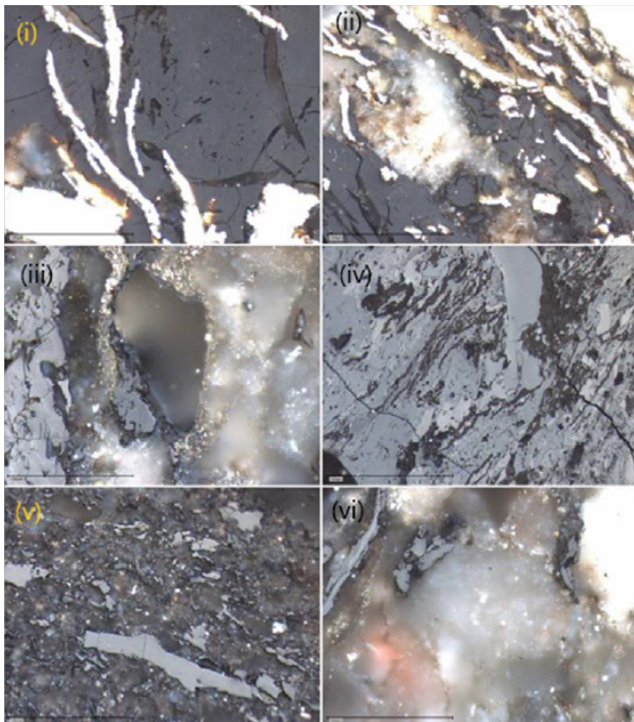


Figure 4—Micrographs of the sink fraction: (i) & (ii) Pyrite and carbonate cleats; in vitrinite, (iii) Sub-angular quartz grain; (iv) inertinite particle with thin liptinite strands and included carbonate minerals; (v) fine quartz and clays; (vi) large quartz grains (reflected light, oil immersion, x500, scale included 100 microns)

remained similar in the feed coal and the  $<1.5 \text{ g.cm}^{-3}$  float fraction, increasing to 62.3 vol.% and 56 vol.% in the  $<1.7 \text{ g.cm}^{-3}$  float fraction and  $<1.9 \text{ g.cm}^{-3}$  float fractions respectively. The content of liptinite, which is a more ductile maceral and thus harder to grind (Trimble and Hower, 2003; Rejda, Micorek, and Hower, 2018), increased from 4 vol.% in the feed coal to 5.9 vol.% in the  $<1.5 \text{ g.cm}^{-3}$  float fraction and decreased to 3.7 vol.% and 1.7 vol.% in the  $<1.7 \text{ g.cm}^{-3}$  and  $<1.9 \text{ g.cm}^{-3}$  float fractions respectively.

When comparing the petrographic results it is evident that there is a decrease in vitrinite and liptinite contents as the density of the organic liquid is increased. This resulted in the highest vitrinite and liptinite contents reporting in the  $<1.5 \text{ g.cm}^{-3}$  float fraction (hard to grind). Furthermore, the  $>1.9 \text{ g.cm}^{-3}$  sink fraction (softest to grind) is characterized by the lowest proportions of inertinite (14.1 vol.%), vitrinite and liptinite (1.2 vol.%), and the highest proportion of mineral matter (80 vol.%). These results are consistent with maceral data of coal samples obtained in previous studies (Rautenbach *et al.*, 2019). Also, the petrographic results of the sink fraction agree with the XRD results of this material in terms of a higher mineral matter content.

## HGI measurements

The HGI values obtained using a standard HGI analysis are depicted in Figure 5. It is clear that the HGI values of the density fractions increase with an increase in the particle density produced from the density separation experiments. The  $<1.5 \text{ g.cm}^{-3}$  float fraction achieved the lowest HGI value of 56.5 (hardest to grind) compared to 68.6 and 62.6 for the feed coal and the  $<1.7 \text{ g.cm}^{-3}$  float fraction respectively. However, the  $>1.9 \text{ g.cm}^{-3}$  sink fraction had the highest HGI value (76), and is thus softest to grind.

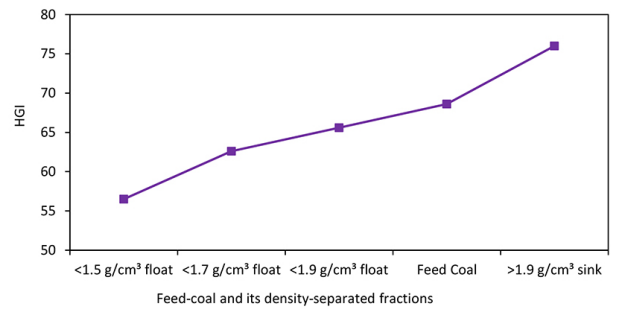


Figure 5—HGI values of feed coal and its density-separated fractions

The higher proportion of total macerals with a higher carbon content as well as a higher proportion of liptinite (6 vol.%, Table V), together with the lower kaolinite content (9%, Table III) present in the  $<1.5 \text{ g.cm}^{-3}$  float fraction are attributed to the hardness of this fraction, which can be linked with the equipment wear during preparation of the PF.

Coals which have lower HGI values grind or pulverize with difficulty and subsequently result in erosion and damage to the plant crushers and pulverizer parts (Falcon and Ham, 1988; Sligar, 1998; Deniz, 2011). Furthermore, these materials require high energy to pulverize. On the other hand, the  $>1.9 \text{ g.cm}^{-3}$  sink fraction with a higher mineral matter content and higher ash yield, as well as a lower macerals content, exhibited the highest HGI value. This fraction can be pulverized or ground with ease to produce PF of poor quality (due to the lower carbon content) without damaging the crusher parts. It has also been reported that Afsin-Elbistan (Turkey) coals or rocks containing higher ash yields, as well as soft mudstone, can be milled very easily (Ürünveren *et al.*, 2017; Bhattarai *et al.*, 2007).

## Coal grinding experiments

The percentage of dried finer particles passing a  $75 \mu\text{m}$  sieve after milling the  $<1000 \mu\text{m} >250 \mu\text{m}$  coal samples (feed coal,  $<1.5 \text{ g.cm}^{-3}$  float fraction,  $<1.7 \text{ g.cm}^{-3}$  float fraction,  $<1.9 \text{ g.cm}^{-3}$  float fraction, and  $>1.9 \text{ g.cm}^{-3}$  sink fraction) for 1 hour are 59.4, 56.4, 58.3, 63.6, and 66.9 respectively.

The  $<1.9 \text{ g.cm}^{-3}$  float fractions and  $>1.9 \text{ g.cm}^{-3}$  sink fraction contain significantly higher mineral matter (Tables III and V) compared to the other samples, which contained higher proportions of  $<75 \mu\text{m}$  particles. This formation of finer particles can be ascribed to the high proportion of mineral matter present, consisting of soft mudstone rock fragments (kaolinite and spherical quartz particles or quartz grains) (Wetzel and Einsele, 1991; Bhattarai *et al.*, 2007), and lower contents of carbon and total macerals (Tables I and V). Also, the  $>1.9$  sink fraction had the highest HGI value, which is associated with the softness of the sink particles. This fraction can thus be milled/ground easily during the grindability experiments without wearing the mill or crusher parts.

Due to higher proportions of total macerals and carbon (Tables I and V) as well as lower mineral matter content (Tables III and V) and a lower HGI value (Figure 5) in the  $<1.5 \text{ g.cm}^{-3}$  float fraction, this sample contained the lowest proportion of  $<75 \mu\text{m}$  particles. Therefore, this fraction contained harder particles which were ground with difficulty during the grindability study. This sample can be linked with the erosion or damage to the crusher or mill parts during the preparation of PF. On the other hand, 40.6, 47.6, 41.7, 36.4, and 33.1% of the coarser particles ( $>75 \mu\text{m}$ ) of the coal samples respectively, were retained on the  $75 \mu\text{m}$  sieve during the wet screening procedure.

# Effect of chemical, mineralogical, and petrographic properties

## Optimization of the grinding time for the $<1.5 \text{ g.cm}^{-3}$ float fraction

From the one-hour milling experiments the  $<1.5 \text{ g.cm}^{-3}$  float was identified as the fraction hardest to grind, which is related to the high proportion of total macerals and carbon. Results show that the percentage of  $<75 \mu\text{m}$  particles increase with an increase in the grinding time (Table VI) with the CV of 27.5 MJ/kg (Table I). This implies that more energy, which is not economically favourable, is required to grind the hard particles present.

The results for the density fractions in this investigation can be used in the coal preparation plant to produce a suitable PF (20–32% ash yield, 0.5–1% total S, 40–55% fixed-carbon, and CV of 15–25 MJ/kg) for feeding to South African boilers.

## PSD analysis

PSD results for the feed coal and density fractions after grinding for 1 hour are depicted in Figures 6. It is apparent that the PSD curves shift to the left-hand side (more fine particles) with increasing grinding time. Thus, the  $>1.9 \text{ g.cm}^{-3}$  sink fraction with a high HGI value, containing significant proportions of mineral matter and ash yield as well as a lower total macerals content, being easier to grind generated significant amounts of finer particles ( $<75 \mu\text{m}$ ) compared to the other samples (Figure 6). Furthermore, the  $<1.5 \text{ g.cm}^{-3}$  float fraction which contained the highest contents of carbon, fixed-carbon, and total macerals and the lowest mineral matter content and ash yield, produced only a small amount of fine particles ( $<75 \mu\text{m}$ ) and retained a higher proportion of coarse particles ( $>75 \mu\text{m}$ ) compared to the  $>1.9 \text{ g.cm}^{-3}$  sink fraction. This sample (Figure 6) is comparatively difficult to grind, which can subsequently contribute to the damage and erosion of equipment during pulverization and result in a low production efficiency due to the energy consumption for grinding as well as more frequent boiler shutdowns.

## Effect of grinding time on PSD of the $<1.5 \text{ g.cm}^{-3}$ float fraction

PSD results for the selected hard ( $<1.5 \text{ g.cm}^{-3}$ ) float fraction with the lowest HGI value pulverized for different times are illustrated in Figure 7. It can be seen that the longer the grinding time, the more the PSD curves shift to the left-hand side of the figure. This means that significant amounts of finer particles ( $<75 \mu\text{m}$ ) are produced after grinding for 120 minutes. As expected, the number of finer particles increases with an increase in the grinding time. Thus, more energy is needed to grind the sample with the lowest HGI value (higher hardness). A lower HGI (hard) coal and a higher HGI (soft) coal should therefore be blended at the optimum ratio to prepare a feedstock for PF production while taking into account the combustibility and reactivity of carbon.

## HGI correlation coefficients ( $R^2$ )

$R^2$  values were calculated for the correlation between the chemical, mineralogical, and petrographic results (Tables I, III, and V) for the feed coal and its density fractions and their HGI values. For example, the inherent moisture content was correlated with the HGI

Grinding time (min)	% $<75 \mu\text{m}$
15	56.4
30	69.1
60	78.5
120	95.6

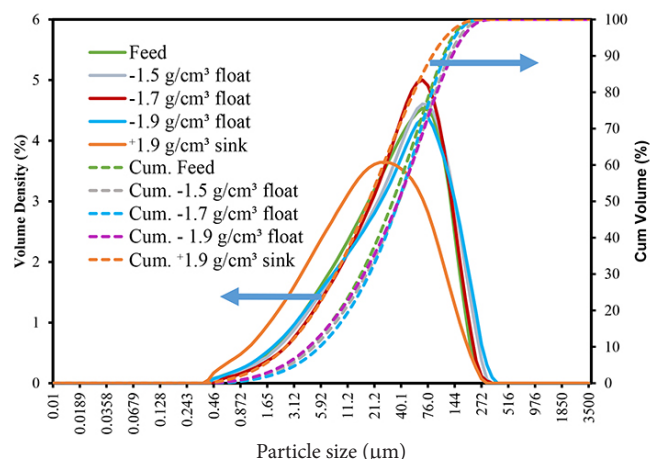


Figure 6—PSD results for coal samples which were milled for 1 hr

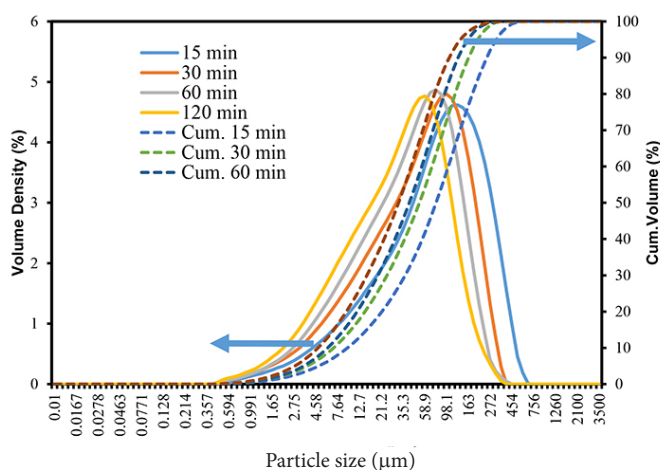


Figure 7—PSD results of the  $<1.5 \text{ g.cm}^{-3}$  float fraction ground at different times

of the coal samples using Results Set 1 of the measured HGI values (Figure 5) and Results Set 2 of the inherent moisture values (Table I), as well as by Equation [1].

$$\begin{aligned} \text{The excel formula for } R^2 & \\ &= \text{RSQ}([\text{Results set 1}], [\text{Results set 2}]) \quad [1] \\ &= \text{SRQ}(56.5:76.0, 3.8:2.1) \\ &= 0.483 \end{aligned}$$

The calculated  $R^2$  values are presented in Figure 8. It can be observed that the inherent moisture (dry) and total sulphur (dry) have minor effects on the HGI values, while ash yield (dry), mineral matter (dry), fixed-carbon (dry), amorphous organic carbon (dry), and total macerals (dry) have significant impacts. Kogut *et al.* (2021) confirmed that the inherent moisture (dry), oxygen (dry), and total sulphur (dry) have the least effects on the HGI values of coals evaluated in their studies, and volatile matter (dry), carbon (dry), hydrogen (dry), nitrogen (dry), and fixed-carbon (dry) have substantial effects.

Sengupta (2002) found that the higher  $R^2$  of 0.94 was achieved with the HGI being correlated with proximate analysis results for coal using a statistical grindability index (SGI). The SGI was found useful for evaluating coal behaviour during the pulverization of coarse coal to produce PF. Idris *et al.* (2022) developed a model



## Effect of chemical, mineralogical, and petrographic properties

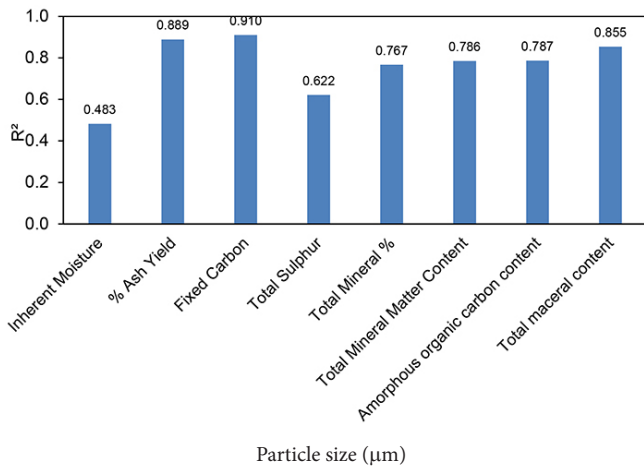


Figure 8—Correlation between input parameters and the measured HGI

that yielded better HGI predictions for blends of low-grade and high-grade coal, with  $R^2 = 0.94$  using proximate, ultimate, and HGI results.

Some soft mudstone particles with associated kaolinite and lower carbon content in the  $>1.9 \text{ g.cm}^{-3}$  sink fraction could possibly be broken or ground with ease to generate more fines or dusts during grinding (Hower, Graese, and Klapheke, 1987; Bhattarai *et al.*, 2007; Wetzel and Einsele, 1991). These sink samples may thus have a higher HGI value. On the other hand, the float samples containing higher proportions of carbon associated with macerals and lower proportions of inherent mineral matter (including kaolinite and quartz) can be harder to grind than the sink fraction. These float fractions are thus postulated to have lower HGI values and a higher organic carbon content, thereby requiring higher energy to grind (Sligar, 1998; Deniz, 2011).

### Conclusions

A range of techniques (proximate and ultimate, sulphur speciation, total sulphur, XRF, XRD, HGI, PSD, and petrology) was used to investigate the effects of chemical, mineralogical, physical, and petrographic properties on the HGI of a feed coal and its density fractions. Factors that are associated with damage to plant equipment were calculated to  $R^2$  values and correlated with the measured HGI, and further time-based grindability tests were conducted.

- Proximate results indicate that the  $>1.9 \text{ g.cm}^{-3}$  sink fraction generated the highest ash yield and mineral matter, and had the lowest contents of fixed-carbon and volatile matter. The  $<1.5 \text{ g.cm}^{-3}$  float fraction contained the highest volatile matter and percentage fixed-carbon compared to the  $<1.7 \text{ g.cm}^{-3}$  and  $<1.9 \text{ g.cm}^{-3}$  fractions. The high volatile matter and fixed-carbon contents, along with the low ash yield, could potentially contribute to the hardness of the  $<1.5 \text{ g.cm}^{-3}$  float fraction as shown in the grindability tests.
- Ultimate analysis results show that the float fraction samples ( $<1.5 \text{ g.cm}^{-3}$ ,  $<1.7 \text{ g.cm}^{-3}$ ,  $<1.9 \text{ g.cm}^{-3}$ ) and the feed coal sample contained higher carbon, nitrogen, and hydrogen than the  $>1.9 \text{ g.cm}^{-3}$  sink fraction.
- The sulphur analysis detected pyrite in the coal particles. Depending on the shape, size, and mode of occurrence of the particles, which are harder than coal, pyrite may contribute to the wearing of equipment during pulverization of the feed coal in preparation for gasification and combustion.

- XRD analysis detected significant proportions of kaolinite and quartz, with lesser proportions of dolomite, pyrite, and calcite and traces of illite, microcline, and anatase in the feed coal and its density fractions. The highest proportions of quartz, kaolinite, and total mineral matter were evident in the  $>1.9 \text{ g.cm}^{-3}$  sink fraction, where they are associated with fragments of soft mudstone, siltstone, and sandstone.
- The  $>1.9 \text{ g.cm}^{-3}$  sink fraction, which had a high mineral matter content and ash yield, as well as a low total macerals content, had the highest HGI value. This material can easily be milled to produce pulverized fuel (PF) of poor quality without damaging the plant crusher parts.
- Due to the high proportions of mineral matter (kaolinite and quartz) in the  $<1.9 \text{ g.cm}^{-3}$  float fraction and  $>1.9 \text{ g.cm}^{-3}$  sink fraction, these samples yielded more finer particles ( $<75 \mu\text{m}$ ) and fewer coarser particles ( $>75 \mu\text{m}$ ) during the laboratory grindability tests. The  $<1.5 \text{ g.cm}^{-3}$  float fraction generated the least finer particles ( $<75 \mu\text{m}$ ) and the highest proportion of coarser particles ( $>75 \mu\text{m}$ ) due to higher contents of total macerals and carbon and lower mineral matter content, which resulted in the lowest HGI value. This fraction contained harder particles which were ground with difficulty. The hardness of these particles can be linked with equipment wear during the preparation of PF.
- Results also show that the percentage of finer particles ( $<75 \mu\text{m}$ ) increases with an increase in the grinding time during the milling of the  $<1.5 \text{ g.cm}^{-3}$  float fraction, while the percentage of coarser particles ( $>75 \mu\text{m}$ ) decreases. More energy, which is not economically favourable, is required to grind these harder  $<1.5 \text{ g.cm}^{-3}$  float fraction particles with higher proportions of total macerals and fixed-carbon.
- PSD results from the milling tests indicate that the  $<1.5 \text{ g.cm}^{-3}$  float fraction (the hardest sample) produced a small number of fine particles and a significant number of coarse particles compared to of the  $>1.9 \text{ g.cm}^{-3}$  sink fraction (the softest sample).
- From the measured HGI results, the calculated  $R^2$  values for inherent moisture, ash yield, and contents of fixed-carbon, total sulphur, total minerals (kaolinite and quartz), total mineral matter, amorphous organic carbon, and total maceral content are 0.48, 0.89, 0.91, 0.62, 0.77, 0.79, 0.79, and 0.85 respectively. Based on the  $R^2$  values, the inherent moisture (dry basis) and total sulphur (dry) have only minor effects on the HGI values. On the other hand, the ash yield, mineral matter, sum of proportions of kaolinite and quartz, fixed-carbon, amorphous organic carbon, and macerals (all on a dry basis) have significant impacts on the HGI values.

These results indicate that in commercial combustion plants, a blending strategy of coals with different mineralogical and petrological properties should be adopted to generate a suitable PF with 20–32% ash yield (a.d.b),  $<0.5\text{--}1\%$  total sulphur (a.d.b), 40–55% fixed-carbon (a.d.b), and calorific value 15–25  $\text{MJ.kg}^{-1}$  with low equipment wear propensity and no influence on the efficiency or erosion of the boiler. It is highly recommended that the effects of the types microlithotypes and macerals on the grinding (HGI) of South African feed coals and their density fractions be studied during pulverization tests.

### Acknowledgements

The authors thank SGS SA (Pty) Ltd laboratories, Secunda for

# Effect of chemical, mineralogical, and petrographic properties

preparation of the coal samples for the experiments at North-West University; in particular Morne van Zyl of SGS laboratories, Prof N. Wagner of the University of Johannesburg, Geology Department, Dr Sabine Verryn of XRD Analytical and Consulting, Mrs. B Venter and the analysts of the School of Chemical and Minerals Engineering, North-West University, as well as SGS analysts for analyses following the proximate, ultimate, sulphur speciation, HGI, XRD, XRF, petrographic, and PSD test work, respectively. The authors acknowledged NWU fourth-year student, Miss Anne Goosen for extracting this manuscript from her research report. The information presented in this paper is based on research financially supported by the SA Research Chairs Initiative (SARChI) of the Department of Science and Technology and the National Research Foundation of South Africa (Coal Research Chair Grant No. 86880). Any opinion, finding, or conclusion or recommendation expressed is that of the authors and the NRF does not accept any liability in this regard.

## References

- BABU, K.A., LAWRENCE, A., and SIVASHANMUGAM, P. 2018. Grindability studies on blended coals of high-ash Indian coals with low-ash imported coals. *International Journal of Coal Preparation and Utilization*, vol. 38, no. 8. pp. 433–442. doi: 10.1080/19392699.2017.1281254
- BHATTARAI, P., MARUI, H., TIWARI, B., WATANABE, N., and TULADHAR, G.R. 2007. "Depth-wise variation of physical and mechanical properties of mudstone in relation to weathering -cases in several landslides in Niigata Prefecture. *Journal of the Japan Landslide Society*, vol. 44, no. 2. pp. 79–89. doi:10.3313/JLS.44.79
- BORREGO, A.G., ALVAREZ, D., and MENENDEZ, R. 1997. Effects of Inertinite content in coal on char structure and combustion. *Energy and Fuels*, vol. 11, no. 3. pp. 702–708.
- DENIZ, V. 2011. Effects of two important parameters on capacity of a laboratory jaw crusher of different coals: Choke feed level and effective reduction ration. *International Journal of Coal Preparation and Utilization*, vol. 31, no. 6. pp. 335–45. doi:10.1080/19392699.2011.576657
- ENGELBRECHT, A.D., EVERSON, R.C., NEOMAGUS, H.W.P.J., and NORTH, B.C. 2010. Fluidized bed gasification of selected South African coals. *Journal of the Southern African Institute of Mining and Metallurgy*, vol. 110. pp. 225–30.
- FALCON, R.M.S. and FALCON, L.M. 1987. The petrographic composition of Southern African coals in relation to friability, hardness, and abrasive indices. *Journal of the Southern African Institute of Mining and Metallurgy*, vol. 87, no. 10. pp. 323–36. doi: 10.10520/AJA0038223X\_1745.
- FALCON, R. and HAM, A.J. 1988. The characteristics of Southern African coals. *Journal of the Southern African Institute of Mining and Metallurgy*, vol. 88, no. 5. pp. 145–161.
- FAURE, K., WILLIS, J. P., and DREYER, J. C. 1996. The Grootegeluk formation in the Waterberg Coalfield, South Africa: Facies, palaeoenvironment and thermal history — Evidence from organic and clastic matter. *International Journal of Coal Geology*, vol. 29, no. 1–3. pp. 147–86. doi: 10.1016/0166-5162(95)00029-1.
- HANSEN, A.E. and HOWER, J.C. 2014. Notes on the relationship between microlithotype composition and Hardgrove grindability index for rank suites of Eastern Kentucky (Central Appalachian) coals. *International Journal of Coal Geology*, vol. 131. pp. 109–112.
- HONAKER, R.Q., MOHANTY, M.K., and CRELLING, J.C. 1996. Coal maceral separation using column flotation. *Minerals Engineering*, vol. 9. pp. 449–464.
- HOWER, J.C., GRAESE, A.M., and KLAPEHEKE, J.G. 1987. Influence of microlithotype composition on Hardgrove grindability for selected eastern Kentucky coals. *International Journal of Coal Geology*, vol. 7. pp. 227–244
- HOWER, J.C., BAGHERIEH, A.H., DINDARLOO, S.R., TRIMBLE, A.S., and CHELGANI, S.C. 2021. Soft modelling of the hardgrove grindability index of bituminous coals: An overview. *International Journal of Coal Geology*, vol. 247. 103846.
- IDRIS, A., MAN, Z., BUSTAM, A., RABAT, N.E., UDDIN, F., and MANNAN, H.A. 2022. Grindability and abrasive behavior of coal blends: Analysis and prediction. *International Journal of Coal Preparation and Utilization*, vol. 42. no. 4. pp. 1143–1169. doi:10.1080/19392699.2019.1694009
- JEFFREY, L. 2005. Challenges associated with further development of the Waterberg Coalfield. *Journal of the South African Institute of Mining and Metallurgy*, vol. 105. pp. 453–457.
- KHOSHJAVAN, S., KHOSHJAVAN, R., and REZA, B. 2013. Evaluation of the effect of coal chemical Properties on the hardgrove grindability index (HGI) of coal using artificial neural networks. *Journal of the Southern African Institute of Mining and Metallurgy*, vol. 113. pp. 505–510.
- KOGUT, K., CABLIK, V., MATUSIAK, P., KOWOL, D., SUPONIK, T., FRANKE, D. M., TORA, B., and POMYKALA, R. 2021. A study on the hard coal grindability dependence on selected parameters. *Energies*, vol. 14. 8158. doi: 10.3390/EN14238158
- MALVERN INSTRUMENTS LTD. 2015. 'Mastersizer 3000 User Manual.' MAN0474-07EN-00.
- MANGENA, S.J. 2001. The amenability of some South African bituminous coals to binders briquetting. MTEch Chemistry. Faculty of natural sciences, Technikon Pretoria, South Africa.
- MATJIE, R.H., VAN ALPHEN, C., and PISTORIUS, P.C. 2006. Mineralogical characterization of Secunda gasifier feedstock and coarse ash. *Minerals Engineering*, vol. 19, no. 3. pp. 256–261. doi:10.1016/J.MINENG.2005.06.010
- MATJIE, R.H., LI, Z., WARD, C.R., BUNT, J.R., and STRYDOM, C.A. 2016. Determination of mineral matter and elemental composition of individual macerals in coals from Highveld mines. *Journal of the Southern African Institute of Mining and Metallurgy*, vol. 116, no. 2. pp. 169–180. doi:10.17159/2411-9717/2016/v116n2a8
- MATJIE, R.H., LESUFI, J.M., BUNT, J.R., STRYDOM, C.A., SCHORBET, H.H., and UWAOMA, R. 2018. *In situ* capturing and absorption of sulfur gases formed during thermal treatment of South African coals. *ACS Omega*, vol. 3, no. 10. pp. 14201–14212. doi:10.1021/ACSEOMEGA.8B01359/ASSET/IMAGES/LARGE/AO-2018-01359M\_0008.JPEG
- NAG, D., DAS, B., SINGH, R., SRIRAMOJU, S., MESHRA, A., and DASH, P.S. 2022. Effect of Grinding Behavior on Liberation of Coal Macerals. *ISIJ International*, vol. 62, no. 1. pp. 99–103. <https://doi.org/10.2355/isijinternational>. ISIJINT-2021-209
- NORRISH, K., and HUTTON, J.T. 1969. An accurate X-ray spectrographic method for the analysis of a wide range of geological samples. *Geochimica et Cosmochimica Acta*, vol. 33, no. 4. pp. 431–453. doi: 10.1016/0016-7037(69)90126-4
- RAUTENBACH, R., STRYDOM, C.A., BUNT, J.R., MATJIE, R.H., CAMPBELL, Q.P., and VAN ALPHEN, C. 2019. Mineralogical, chemical, and petrographic properties of selected South African power stations' feed coals and their corresponding density-separated fractions using float-sink and reflux classification methods. *International Journal of Coal Preparation and Utilization*, vol. 39, no. 8. pp. 421–446. doi:10.1080/19392699.2018.1533551
- REJDAK, M., MICOREK, T., and HOWER, J.C. 2018. Influence of selected factors of Polish coking coals on the Hardgrove grindability index (HGI). *International Journal of Coal Preparation and Utilization*, vol. 41, no. 11. pp. 789–802. doi:10.1080/19392699.2018.1526790
- RIETVELD, H.M. 1969. A profile refinement method for nuclear and magnetic structures. *Journal of Applied Crystallography*, vol. 2, no. 2. pp. 65–71. doi: 10.1107/S0021889869006558.
- SENGUPTA, A.N. 2002. An assessment of grindability index of coal. *Fuel Processing Technology*, vol. 76, no. 1. pp. 1–10. doi: 10.1016/S0378-3820(01)00236-3
- SHAHZAD, M., IQBAL, M.M., HASSAN, S.A., SAQIB, S., and WAQAS, M. 2014(a). An assessment of chemical properties and hardgrove grindability index of Punjab coal. *Pakistan Journal of Scientific and Industrial Research Series A; Physical Sciences*, vol. 57, no. 3. pp. 139–144.
- SHAHZAD, K.S., KANWAL, S., NAWAZ, N., SHEIKH., and MUNI, S. 2014(b). Effects of moisture and coal blending on the hardgrove grindability index of Pakistani coals. *International Journal of Coal Preparation and Utilization*, vol. 34. pp. 1–9. doi:10.1080/19392699.2013.776961
- SLIGAR, J. 1998. The Hardgrove grindability index. <https://www.acarp.com.au/Media/ACARP-WP-5-HardgroveGrindabilityIndex.pdf>.
- SPEAKMAN, S.A. 2012. Introduction to PANalytical X'Pert HighScore Plus v3.0. MIT Center for Materials Science and Engineering. <http://prism.mit.edu/xray/HighScore%20Plus%20Guide.pdf>
- STEYN, M., and MINNITT, R.C.A. 2010. Thermal coal products in South Africa. *Journal of the Southern African Institute of Mining and Metallurgy*, vol. 110. pp. 593–599.
- TIRYAKI, B. and DIKMEK, A.C. 2005. Effects of rock properties on specific cutting energy in linear cutting of sandstones by picks. *Rock Mechanics and Rock Engineering*, vol. 39, no. 2. pp. 89–120. doi: 10.1007/S00603-005-0062-7
- TRIMBLE, A.S., and HOWER, J.C. 2003. Studies of the relationship between coal petrology and grinding properties. *International Journal of Coal Geology*, vol. 54. pp. 253–260.
- TSEMANE, M.M., MATJIE, R.H., BUNT, J.R., NEOMAGUS, H.W.J.P., STRYDOM, C.A., WAANDERS, F.B., VAN ALPHEN, C., and UWAOMA, R. 2019. Mineralogy and petrology of chars produced by South African caking coals and density-separated fractions during pyrolysis and their effects on caking propensity. *Energy and Fuels*, vol.33, pp. 7645–7658.
- ÜRÜNVEREN, A., ALTINER, M., KUVVETLI, Y., URAL, O.B., and URAL, S. 2020. Prediction of hardgrove grindability index of Afsin-Elbistan (Turkey) low-grade coals based on proximate analysis and ash chemical composition by neural networks. *International Journal of Coal Preparation and Utilization*, vol. 40, no. 10. pp. 701–711. doi:10.1080/19392699.2017.1406350
- VAN VUUREN, M.C.J. 1978. A Survey of the hardgrove grindability indices from colliery product samples. *Fuel Research Institute of South Africa*, vol. 62. pp. 57–68.
- VRANJES, S., MISCH, D., SCHOBERL, T., KIENER, D., GROSS, D., and SACHSENHOFER, R.F. 2018. Nanoindentation study of macerals in coals from the Ukrainian Donets Basin. *Advances. In Geosciences*, vol. 45. pp. 73–83.
- WETZEL, A. and EINSELE, G. 1991. On the physical weathering of various mudrocks. *Bulletin of the International Association of Engineering Geology*, vol. 44. pp. 89–100. doi: 10.1007/BF02602713